TERMINAL VOLTAGE STABILIZATION OF PELLETRON TANDEM ACCELERATOR

Nikolai R. Lobanov#, Dimitris Tsifakis, Peter Linardakis, Michael Blacksell, The Department of Nuclear Physics, Research School of Physics and Engineering, The Australian National University, Canberra, Australia

Abstract

An NEC terminal voltage stabiliser TPS-6.0, based on conventional corona control, has been installed and investigated on the ANU 14UD tandem accelerator. The fluctuations in the charge transport of the electrostatic pelletron generator and their correlation with mechanical oscillations of the chains and terminal voltage ripple have been analysed. Emphasis during commissioning is placed on the components of the two-loop feedback system and on the application of this system to production of high energy-resolution beams. The relationship between transfer functions for the two loops required for optimum operation is discussed. This system produces the beam position at the image slit of the 90° energy-analysing magnet with long-term stability equivalent to a 3.9 kV FWHM fluctuation of the terminal voltage. The concept of novel fast control loop utilizing the high-frequency component from the image slits to control the voltage of the last gap of high-energy acceleration tube is described.

INTRODUCTION

A variety of nuclear physics experiments require the minimum energy spread of particle beams. High-energy resolution is also required for the need in beam position stability at applications of ion beam analyses. Several methods have been employed to achieve beam energy resolutions of $\Delta E/E = 10^{-4}$ to 10^{-5} in the electrostatic accelerators. In small machines with a terminal voltage below 5 MV, the stabilization system can be implemented by controlling the up-charging voltage [1]. The modulation of the amplitude of down-charge has a more rapid effect on the terminal voltage than corresponding changes in up-charge. The Daresbury 30 MV tandem has used the laddertron down-charge with the response speed limited to 0.06 s delay [2]. Burger *et al.* refer to the stable periodic pattern of the acceleration voltage fluctuations and have introduced "predictive fluctuation compensation" [3]. A TUNL system has implemented the terminal collector filter circuit for charging system [4]. The potential of the terminal can be controlled by varying the current load [1]. A fast response variation is achieved by modulating the electron beam from a gun at a base of the tube.

Since the weak components of the control loop are the signal delay characterizing the corona transfer function and the response of down-charge or variable load systems, a more direct energy-affecting element with fast response is desirable. The components for the application of the corrective voltages are the ion source, the terminal or the stripper, the high energy end of the accelerator and the target. Reference [1] describes a terminal ripple reduction system consisting of a capacitive liner along the tank wall facing the terminal, to which a terminal correction voltage derived from a capacitive pick-up or slit current signal is applied. Modulating the terminal stripper is another alternative [5]. The energy of the particles at the terminal is high enough so that a few kV energy modulation does not affect the optics. At a number of laboratories, various techniques such as time of flight, data gating, energy sorting and target potential modulation are being used to improve the energy resolution.

We will describe an energy feedback system yielding high-resolution particle beams, which has been developed for the ANU Heavy Ion Accelerator Facility (HIAF). This system utilizes two principal feedback mechanisms. The standard feedback loop employs a correction signal derived from summing the signal from capacitive pickoff plates (CPO) with a slit difference signal or a generating voltmeter (GVM). This signal is applied to the control grid of a high voltage triode 6BK4 connected to corona points mounted inside the tank. The maximum cut-off control frequency is below 10 Hz because of the transit time for electrons from the corona points to the terminal. Since information about higher frequency beam energy variations is present in the slit difference signal, t correction voltage is generated and applied to the last gap of the high-energy acceleration tube. This new method has the same advantage as modulation of terminal stripper. However it is much simpler since the control element is located at ground potential. The fast correction loop has not been implemented yet and is at R&D stage. In this paper, we will describe elements of both systems, its application for the production of high-resolution particle beams and some measurements of system performance.

DESCRIPTION OF THE HIAF VOLTAGE CONTROL SYSTEM

The GVM signal is only capable of showing relatively slow voltage variations (<1 Hz) due to the dc filtering of the ac signal generated as the grounded rotating vane alternately covers and uncovers the stator plates connected to the GVM amplifier. The momentum analysed currents intercepted by the control slits at the image position are fed into two matched low-noise logarithmic pre-amplifiers. The slit signals are coupled to the pre-amplifier by short 2 m coaxial cables. The

*Work supported by Heavy Ion Accelerators Education Investment Fund
#Nikolai.Lobanov@anu.edu.au

bandwidth of the pre-amplifier depends on the input current and it is approximately 250 Hz at 100 nA or 5 kHz at 1 µA. Therefore, the slit current amplifier has a relatively low bandwidth for low slit currents. The dc response is characterized by logarithmic gain in the range of 1 nA to 100 µA.

To allow for faster error correction, it has been standard practice to use CPO plates to feed back faster error signals to the TPS. An adjustable crossover frequency determines the frequency above which the CPO error signal takes over from the GVM or slit error signals. All experimental data presented in this work was produced at a crossover frequency set at about 1 Hz.

The conventional corona regulator is used to correct for the large, low-frequency fluctuations in the terminal voltage that are characteristic of the pelletron charging system. The GVM signal is used to maintain the dc terminal voltage in the absence of the slit difference signal. Automatic switching from slit to GVM control is provided when a beam is not present. The CPO provides an ac error signal that may be summed with either the GVM signal or the slit difference signal to reduce low frequency fluctuations in the terminal voltage. The main controller is located in the 14UD control console. The Corona Probe Controller (CPC), CPO and GVM pre-amplifiers are located in the middle of the accelerator tower close-by to the actual devices. The slit difference pre-amplifier is located under the tank next to the slits.

THE OPEN LOOP FREQUENCY RESPONSE

The measurement of open-loop frequency response and phase shift for 14UD corona regulator was made by exciting the corona triode grid with a signal generator and frequency synthesizer, and observing the resulting signal on a GVM [6]. The reason for using the Frequency Synthesizer was to generate very slow frequencies that the Signal Generator could not maintain with a degree of stability. A chart recorder was used to record the slow response to a step function, as no oscilloscope could be found that had an appropriate time base. The step input measurements were used to measure the 1/e time of the accelerator at different terminal voltages, as shown in figure 1.The step function was kept constant at 1 V for these measurements.

The step function was also used to measure the time difference between changing the triode grid voltage and the resulting response in the terminal voltage, as shown in figure 2. This technique is accurate enough to measure transit time when the terminal potential is positive and the charge transport is caused mainly by negative ions.

A similar delay time has been measured by using phase shift method. This method is based on measurement of the phase shift Φ between the GVM output and the sinusoidal signal of frequency f applied to the regulating triode grid.

The sine wave measurements were used to plot the phase and voltage response to frequency at a terminal voltage of 14 MV. The transfer function was measured over the frequency range 0 to10 Hz.

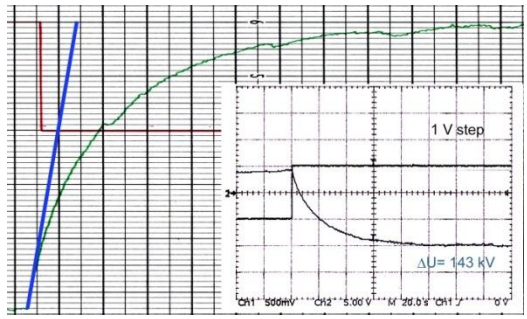

Figure 1: Open-loop response at 8 MV with a 1 V Step Input (red line). The straight blue solid line is the tangent to the GVM signal (green line). Time constant τ_c was 10.2 s. The inset shows the same response captured with the oscilloscope.

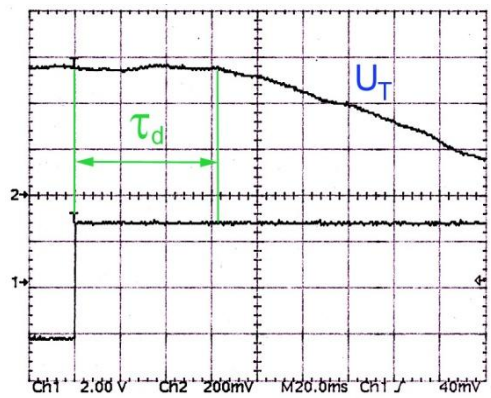

Figure 2: Terminal voltage change with a 1 V Step Input. Measured delay time τ_d =31 ms.

The last set of step measurements were used to estimate the maximum response time of the accelerator at 14 MV. Figure 3 shows the measured open loop voltage response for 14UD corona regulator.

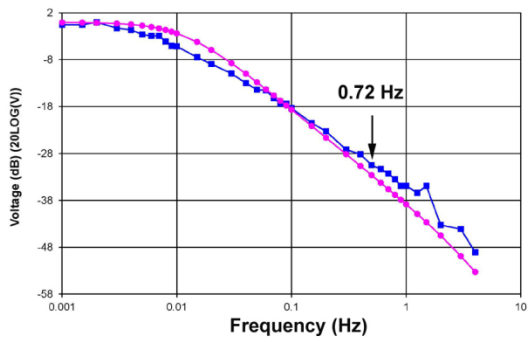

Figure 3: Corona regulator voltage response and curve fitting. Square box is the measured accelerator voltage response; circle is the voltage response calculated from curve fitting equation. 0.72 Hz is the rotation frequency of the chain.

The phase response of the accelerator is shown in figure 4. As shown in figure 2, the 14UD accelerator has a constant 31 ms delay between the triode grid changing and a voltage change appearing on the terminal. The delay depends on the tank SF_6 gas pressure and the position of the corona needles. The closer the needles are to the terminal, the smaller the delay. The measured phase response, figure 4, has the 31 ms delay removed.

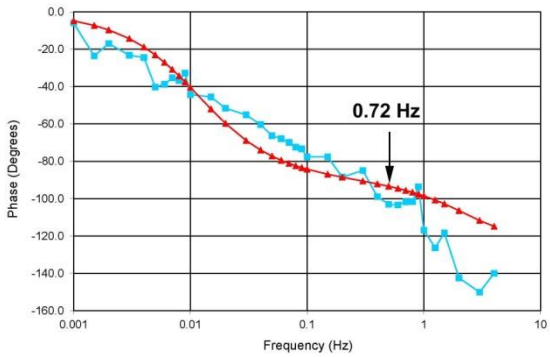

Figure 4: Corona regulator phase response and curve fitting. Square box is the measured accelerator phase response; triangle is the phase response of curve fitting equation. 0.72 Hz is the rotation frequency of the chain.

Using the curve fitting software an equation was found that matched the measured voltage and phase response in the Laplace domain. This program was used to weight the match equally between the phase and voltage. The final Least Squares Error was 4.05353. The equation is shown below:

$$G_p(s) = (1.0 + 0.01s)/(22.6271s^2 + 85.2377s + 1.0) \quad (1)$$

The voltage and phase plots derived from equation (1) fit the measured characteristics of the accelerator adequately, as shown in figures 3 and 4. A black arrow on the Bode plots in figures 3 and 4 marks the frequency 0.72 Hz, which corresponds to the rotation period of the chain. Chains No. 2 and No. 3, installed recently in the tandem, are found to be stimulating the feedback loop into low level oscillation at rotation frequency of the chain. It has been shown subsequently that both chain assemblies have up to 60 degrees torsion twist, causing a mechanical disturbance at each revolution. A stability requirement for a corona regulator is that for all frequencies for which the open loop gain is greater than unity, the accumulated phase shift around the loop must be less than 180° by a phase margin of ~30-40° in practical systems. Evaluation of figure 4 indicates that unity gain for the corona loop is still available at or below 10 Hz at 14 MV terminal voltage, corresponding to given corona points position and ~104 psi pressure of SF_6 gas.

CONTROL SYSTEM PERFORMANCE

The nature of the error signals can be examined with and without the feedback control loop. Figure 5 contains captured traces of the data logger showing the terminal fluctuations measured with CPO and the GVM devices. The two CPO probes are mounted on opposite sides of the terminal in order to minimize the effect of terminal vibrations on the $CPO_\Sigma=CPO_1+CPO_2$ signal.

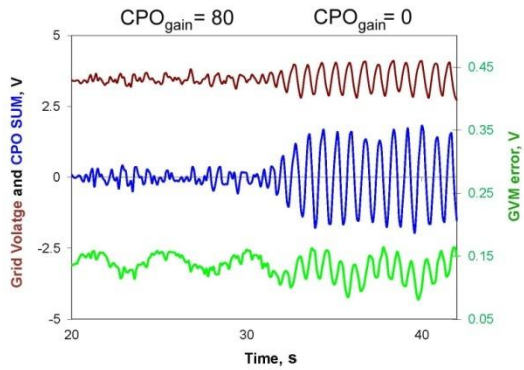

Figure 5: Data logger traces showing grid voltage, CPO_Σ and GVM error signals without and with CPO feedback.

In figure 5, the CPO gain reduced from optimum to 0 ~32 seconds after starting data logging. The controller crossover frequency was set at 0.9 Hz for all experiments. The logger trace gives the slow variations of the measured signal. The trace on the right was taken with the CPO feedback off, the terminal voltage at 13.5 MV and 125 nA of $^{12}C^{+5}$ beam on the stop Faraday cup positioned after energy analysing slits. The trace on the left was taken under the same conditions, except that the CPO feedback was on and the gain was adjusted to minimize the slit error signal. In the left trace, the error signal has been greatly diminished. Figure 6 displays the terminal voltage distribution over a period of about 1 hour at 13.5 MV, with both control and CPO gains set to optimum values.

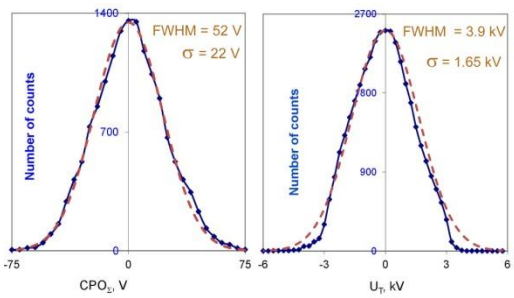

Figure 6: The terminal voltage distribution over a period of about 1 hour. The solid blue line is the output signal from TPS controller. The brown broken line is the normal distribution fit. Both control and CPO gain are set to optimum value. The left image is the CPO_Σ voltage illustrating quick variation of the terminal voltage. The right image is the GVM error signal. It is assumed that FWHM~2.35σ.

The voltage variation plot was obtained by connecting the calibrated CPO preamp output and GVM error output to a bipolar 12 bit data logger. The CPO has been

calibrated so that a 1 V output is equivalent to a 100 V variation in the terminal potential. The GVM error has been calibrated so that a 1 V output is equivalent to a 100 kV variation in the terminal potential. The GVM-controlled terminal voltage deviation, ΔU, as a function of terminal voltage, U_T, is given by equation [1] $\Delta U_{[V]} = 133 U_T$[MV]. One can expect ΔU = 1.8 kV FWHM at U_T = 13.5 MV. From calibration of the system, one can estimate that the fast terminal voltage ripple with the closed loop control is approximately 52 V FWHM and the slow voltage variation is as high as 3.9 kV FWHM.

The measured performance of the control system is below the expected voltage deviation of 1.8 kV FWHM and it may be caused by cross-talk in the energy-analysing slits. Examination of the slit signals showed that secondary electrons were collected alternately by one slit and then another as the beam shifted across it. This effect displayed a threshold behaviour, producing a nearly square wave output at the slit difference amplifier, as shown in figure 7 on the left bottom oscillogram. The same effect was reported in reference [7], where even as much as 3 kV of suppression voltage was not sufficient to eliminate this behaviour. The image slits at HIAF are not designed with minimization of cross-talk in mind. For instance, the shape of the slit electrodes is cylindrical, which is inferior to sharp edges in terms of avoiding secondary electrons from one slit hitting the other. In addition, the reduction of the cross-talk can be achieved by separation of the slits along the beam axis, fitting slits inside the cage and applying electron suppression voltage.

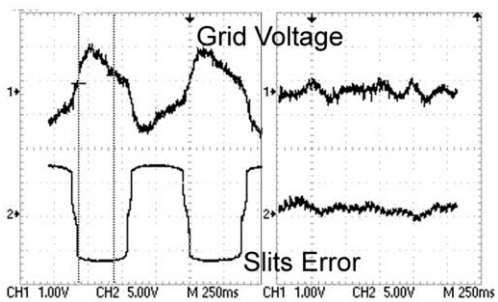

Figure 7: The oscillograms of square wave output at the slit difference amplifier and grid voltage displaying a threshold pattern. The effect is more evident when operating with no CPO control gain as shown on left images. On the right images the same signals are shown with CPO feedback on.

The energy resolution available with this system depends on several factors including the control slit separation and quality of the beam focus at the slit position. The choice of stripper and ion beam are also very important. For the best resolution, it is necessary to use gas stripping as opposed to carbon stripper foils, and light projectile ions to reduce energy straggling of the beam. This system has also been used successfully with bunched and chopped beams.

ONGOING DEVELOPMENT WORK ON THE FAST CONTROL LOOP

We are continuing to improve on the design of main components in energy stabilization system. R&D on the development of the fast control loop in ongoing. When in slit control, the difference of the two control slit currents is summed with the CPO signal. The detected error signal is converted to a dc level and applied to the voltage control tube (6BK4) grid through the high-pass filter with the cut-off frequency of 10 Hz. The same signal is applied to the CPC triode through the low-pass filter. The fast control loop tube is mounted under the tank at the high-energy end of the accelerator and its anode is electrically connected to the last gap of high-energy (HE) acceleration tube. The cathode of the tube is connected to ground. The conductor enters the 14UD tank through a high pressure, high voltage feed-through. The fast control system amplifier response exhibits corner frequencies near 10 Hz and 1 kHz. The low frequency roll-off is important to avoid competition between the slow corona control system, ranging from dc to approximately 10 Hz, and the fast control loop.

In order to implement the fast control loop, the bandwidth of slit difference amplifier is to be increased up to 1 kHz at 10 nA. This method has a direct effect on the output energy without the phase shift inherent with the corona stabilization system. It is expected that a combination of the power of the corona system at low frequency and the speed of the HE tube modulator at high frequency will prove a very powerful stabilisation system.

Another implementation option of the system is to employ the standard NEC controller TPS7.0 with the capability of driving the liner. However in our case the correction voltage is applied to the acceleration gap rather to the liner electrode.

CONCLUSIONS

The beam energy spread and overall performance of the tandem accelerator has been investigated. The standard corona stabilization system provides adequate energy resolution and steady beam on target. The performance can be significantly improved with the addition of a fast feedback system. The proposed system can be easily incorporated into existing corona control system. Beam energy spreads in the range 3.9 kV FWHM are routinely produced. Even where high resolution beams are not required, the additional feedback loop is useful in stabilizing accelerated and momentum analysed dc or pulsed beams on targets or at injection point to post-accelerator.

ACKNOWLEDGEMENT

The authors wish to thank the engineering and technical staff from Electronics Unit RSPE for their help in installation and preliminary tests of the new controller. The authors thank David Weisser for many useful discussions.

REFERENCES

[1] J.A.Ferry, Recent developments in electrostatic accelerator technology at NEC, Nuclear Physics and Methods in Physics Research A328 (1993) 28.

[2] T.W.Aitken, A laddertron modulation system to correct a repetitive charging pattern, Nuclear Physics and Methods in Physics Research A268 (1988) 422.

[3] W. Burger, H.Lange, V.Petr, A new method of improving the acceleration voltage stability of Van de Graaff accelerators, Nuclear Physics and Methods in Physics Research A586 (2008) 160.

[4] C.R.Westerfeldt, E.P.Carter, R.O'Quinn, Modifications to belt and chain charging systems at TUNL, in SNEAP XXXIV, University of Lund, Sweden, 2001, p.141.

[5] R. Hellborg (Ed.), Electrostatic Accelerators, Springer, Berlin, Heidelberg, 2005.

[6] W. Trenchuk, M. Blacksell, Design of an electrostatic accelerator control system, Engineering project, FISE, University of Canberra, 1988

[7] J.E.Cairns, M.W.Greene, J.A.Kuehner, A terminal stabilizer for a tandem accelerator, Nucl.Instrum. and Meth., 114 (1974) 489.